LETTERS

Origin of a 'Southern Hemisphere' geochemical signature in the Arctic upper mantle

Steven L. Goldstein[1,2], Gad Soffer[1,2]†, Charles H. Langmuir[3], Kerstin A. Lehnert[1], David W. Graham[4] & Peter J. Michael[5]

The Gakkel ridge, which extends under the Arctic ice cap for ~1,800 km, is the slowest spreading ocean ridge on Earth. Its spreading created the Eurasian basin, which is isolated from the rest of the oceanic mantle by North America, Eurasia and the Lomonosov ridge. The Gakkel ridge thus provides unique opportunities to investigate the composition of the sub-Arctic mantle and mantle heterogeneity and melting at the lower limits of seafloor spreading. The first results of the 2001 Arctic Mid-Ocean Ridge Expedition (ref. 1) divided the Gakkel ridge into three tectonic segments, composed of robust western and eastern volcanic zones separated by a 'sparsely magmatic zone'. On the basis of Sr–Nd–Pb isotope ratios and trace elements in basalts from the spreading axis, we show that the sparsely magmatic zone contains an abrupt mantle compositional boundary. Basalts to the west of the boundary display affinities to the Southern Hemisphere 'Dupal' isotopic province[2], whereas those to the east—closest to the Eurasian continent and where the spreading rate is slowest—display affinities to 'Northern Hemisphere' ridges. The western zone is the only known spreading ridge outside the Southern Hemisphere that samples a significant upper-mantle region with Dupal-like characteristics. Although the cause of Dupal mantle has been long debated, we show that the source of this signature beneath the western Gakkel ridge was subcontinental lithospheric mantle that delaminated and became integrated into the convecting Arctic asthenosphere. This occurred as North Atlantic mantle propagated north into the Arctic during the separation of Svalbard and Greenland.

The Gakkel ridge is the global ultraslow endmember among ocean ridges, with spreading rates decreasing from ~15 mm yr^{-1} (full rate) at the Lena trough near Greenland to ~6 mm yr^{-1} at the Siberian margin. It contains no significant transform offsets, which on other ridges often form mantle flow and mantle compositional boundaries. It thus provides a natural laboratory in which to study source heterogeneity and melting dynamics at ultraslow spreading rates, and where potential complications from tectonic offsets are absent. Here we report isotope and trace element data on basaltic glasses that document the Arctic mantle composition and processes contributing to its enrichment.

Prior to the 2001 Arctic Mid-Ocean Ridge Expedition, data on Gakkel lavas were restricted to three samples of basaltic cobbles and glass shards recovered on two cruises[3]. The Arctic Mid-Ocean Ridge Expedition collected samples from the western ~850 km of the ridge between longitudes 7° W and 86° E at over 200 stations. Michael *et al.*[1] divided the studied segments into three 'magmato-tectonic zones': the ~200-km-long, shallow, magmatically robust western volcanic zone (WVZ), characterized by normal ocean-ridge-rift magmatism; the ~300-km-long, deep, magma-starved sparsely magmatic zone (SMZ) with peridotite outcropping along the ridge axis; and the ~400-km-long, magmatically robust eastern volcanic zone (EVZ), where axial magmatism is mainly associated with central volcanoes. On the basis of cruise chemical data, Michael *et al.*[1] inferred compositionally distinct mantle beneath the WVZ and the EVZ, with marked barium enrichments in WVZ lavas. Dick *et al.*[4] compared the broad-scale tectonic features of the Gakkel and southwest Indian ridges and posited the existence of a new class of ultraslow-spreading ocean ridge, where 'amagmatic' segments like the SMZ are a consequence of spreading rates less than ~12 mm yr^{-1}, and are thus independent of mantle composition.

Our data confirm fundamental differences in the upper-mantle sources of WVZ and EMZ lavas (locations and data tables can be found in the Supplementary Information). The fields formed by Nd–Sr isotopes of EVZ and WVZ lavas show no overlap (Fig. 1a), and samples from the western and eastern parts of the SMZ show affinities to the adjacent EVZ and WVZ. EVZ lavas have higher $^{143}Nd/^{144}Nd$ values than do WVZ lavas and lower $^{87}Sr/^{86}Sr$ values than does any mid-ocean-ridge basalt (MORB) north of Iceland.

The contrasting WVZ and EVZ mantle compositions are shown in Fig. 1b in terms of Δ8/4 (ref. 2), which reflects deviations from typical compositions of Pacific and Atlantic MORB on $^{208}Pb/^{204}Pb$–$^{206}Pb/^{204}Pb$ diagrams. The disparities also show in along-axis plots of the other radiogenic isotopes (see, for example, Supplementary Fig. 1a). West of the boundary virtually all Gakkel lavas have Δ8/4 > 30; this was shown by Hart[2] to be a primary feature of the Southern Hemisphere 'Dupal isotope anomaly' in Indian and some South Atlantic MORB. The Dupal-like character of the WVZ is further illustrated by comparison with global MORB: $^{208}Pb/^{204}Pb$–$^{206}Pb/^{204}Pb$ data for WVZ basalts lie in the field of Indian MORB (Fig 2a; Supplementary Fig. 2a). WVZ lavas also show a near-vertical trend in a $^{87}Sr/^{86}Sr$–$^{206}Pb/^{204}Pb$ diagram, reflecting a large range of $^{87}Sr/^{86}Sr$ values, typical of Indian MORB, whereas EVZ lavas show a shallow trend similar to that of Atlantic–Pacific basalts (Fig. 2b). Additional evidence of the WVZ's Dupal-like character is given in Supplementary Information (Supplementary Fig. 3).

Gakkel WVZ lavas, however, differ from Southern Hemisphere Dupal basalts, in that they have low Δ7/4 values[2]; their data lie near Atlantic–Pacific basalts on this diagram (Supplementary Fig. 2b). The $^{207}Pb/^{204}Pb$–$^{206}Pb/^{204}Pb$ relationships are temporal rather than a result of the formation process, because they depend primarily on the timing of major U–Pb fractionation, whereas Δ8/4 reflects the chemical composition (Th/U) and the formation age. Oceanic basalts with enriched isotopic signatures (high Sr and low Nd and Hf isotope ratios, and high Δ8/4 values) are associated with both high and low

[1]Lamont-Doherty Earth Observatory of Columbia University, [2]Department of Earth and Environmental Sciences, Columbia University, 61 Route 9W, Palisades, New York 10964, USA. [3]Department of Earth and Planetary Sciences, Harvard University, 20 Oxford Street, Cambridge, Massachusetts 02138, USA. [4]College of Ocean and Atmospheric Sciences, Oregon State University, Corvallis, Oregon 97331, USA. [5]Department of Geosciences, University of Tulsa, 600 South College Avenue Tulsa, Oklahoma 74104, USA. †Present address: Harvard Business School, Soldiers Field, Boston, Massachusetts 02163, USA.

Δ7/4 values (ref. 5), reflecting old and young formation ages, respectively. The Gakkel data thus indicate that the formation of the Arctic Dupal-like source was more recent than that of the Southern Hemisphere Dupal basalts. Although the formation ages differ, chemical characteristics are similar: like Indian MORB, the high Δ8/4 and $^{87}Sr/^{86}Sr$ values reflect high time-integrated Th/U and Rb/Sr values for the Pb and Sr in the lavas, indicating the distinctive chemical compositions of reservoirs responsible for Dupal features.

A striking feature of the Gakkel ridge is the abruptness of the isotopic boundary and its location in the middle of the SMZ (Fig. 1b; Supplementary Fig. 1a). The discontinuity is reminiscent of the Australian–Antarctic discordance of the southeast Indian ridge, which demarcates the boundary between the Indian Dupal and Pacific mantle provinces[5]. Common features include great bathymetric depths and low magma production, as reflected by the basaltic crust being thin in comparison with that of adjoining segments. These indicate close relationships between seafloor structure, bathymetry and mantle convective processes. However, the Gakkel SMZ, unlike the Australian–Antarctic discordance, is not associated with any significant ridge offset. Along a continuously spreading ridge, lavas with isotopic affinities to the WVZ or EVZ were collected within 40 km of each other at longitudes 12.7° E and 16.0° E. The Gakkel SMZ data thus indicate a sharp geochemical boundary in the absence of any tectonic boundary. The Knipovich ridge to the southwest of the Gakkel ridge is also isotopically distinct from the WVZ (see, for example, Supplementary Figs 1b, 2a and 3a), but these ridges are separated by a 600 km offset. The marked change in the magmatotectonic character at the Gakkel SMZ is therefore not simply a tectonic reflection of ultraslow seafloor spreading, as proposed by Dick *et al.*[4], but reflects a mantle compositional and convective boundary.

Comparison with global MORB (Fig. 2) shows that the Pb–Sr–Nd isotope variations in this small Arctic region mimic the global upper-mantle variability. The Gakkel ridge is far from the Indian Ocean. Although enriched MORBs are found along North Atlantic ridges

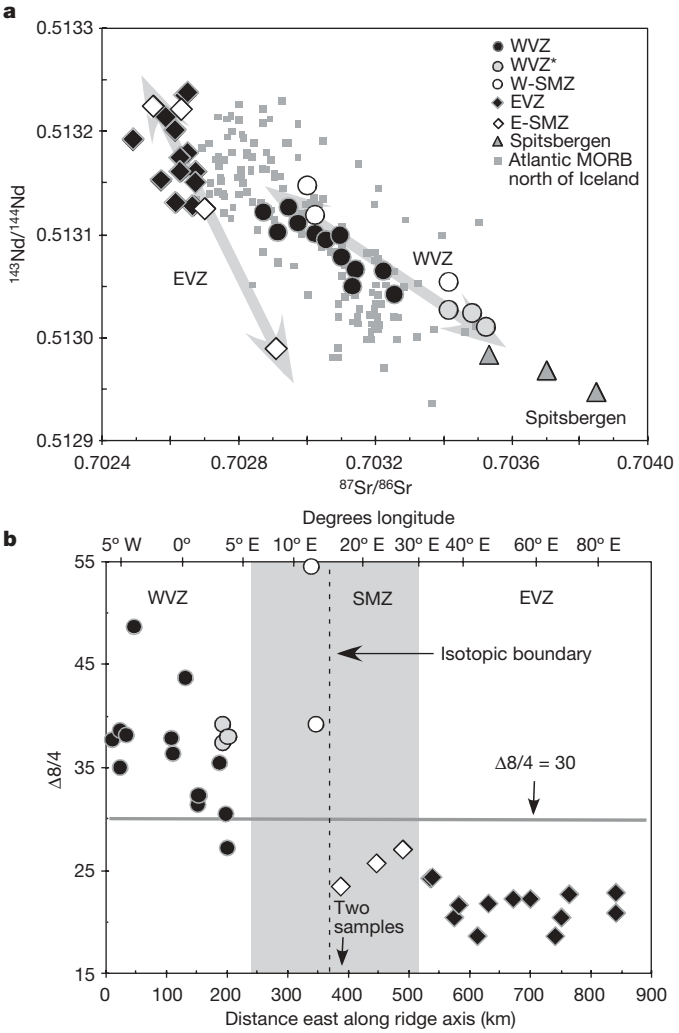

Figure 1 | Distinct western and eastern geochemical provinces in Gakkel ridge basalts. a, $^{143}Nd/^{144}Nd$ versus $^{87}Sr/^{86}Sr$. Data fields for EVZ and WVZ lavas do not overlap. WVZ lava data points overlap with those for Atlantic MORBs north of Iceland and display a trend towards those for Spitsbergen Quaternary-period alkaline basalts. SMZ lavas show affinities to those in the adjacent WVZ and EVZ. W-SMZ and E-SMZ refer to lavas in the SMZ having isotopic affinities to the WVZ and EVZ, respectively. **b**, Δ8/4 (representing deviations from the Northern Hemisphere reference line[2]) versus distance from the western end of the Gakkel ridge near Greenland. (The key is the same as that in **a**.) This shows the distinct WVZ and EVZ compositions and the position and abruptness of the isotopic boundary. Three samples, labelled WVZ*, from near the WVZ–SMZ boundary have unusual chemistry (low SiO_2 and incompatible element abundances, and positive Eu and Sr anomalies on trace element diagrams) and follow the WVZ isotope trend (**a**) but not the WVZ chemical trends (Fig. 3).

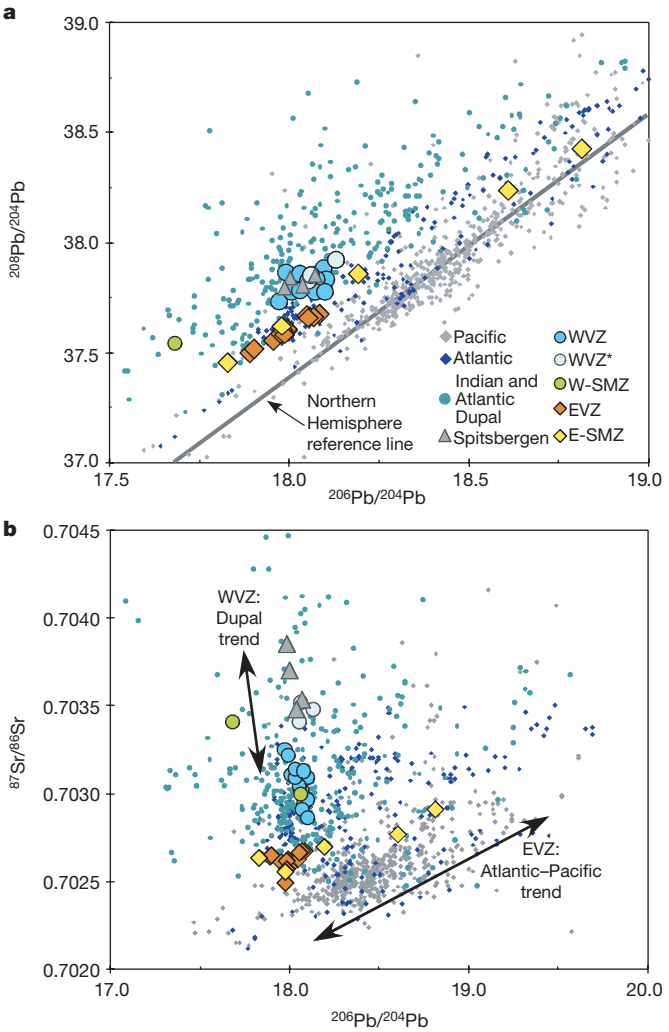

Figure 2 | Gakkel basalts as a microcosm of global MORBs. a, $^{208}Pb/^{204}Pb$ versus $^{206}Pb/^{204}Pb$. WVZ and Spitsbergen lavas show the characteristic Dupal MORB offset to high $^{208}Pb/^{204}Pb$. Global MORB data are from the Petrological Database of the Ocean Floor (www.petdb.org). **b**, $^{87}Sr/^{86}Sr$ versus $^{206}Pb/^{204}Pb$. (The key is the same as that in **a**.) EVZ lavas display a trend similar to that of Atlantic-Pacific MORBs, whereas WVZ MORBs display a near-vertical trend similar to Indian and South Atlantic MORBS showing the Dupal anomaly. The WVZ data points display a trend towards those for Spitsbergen lavas.

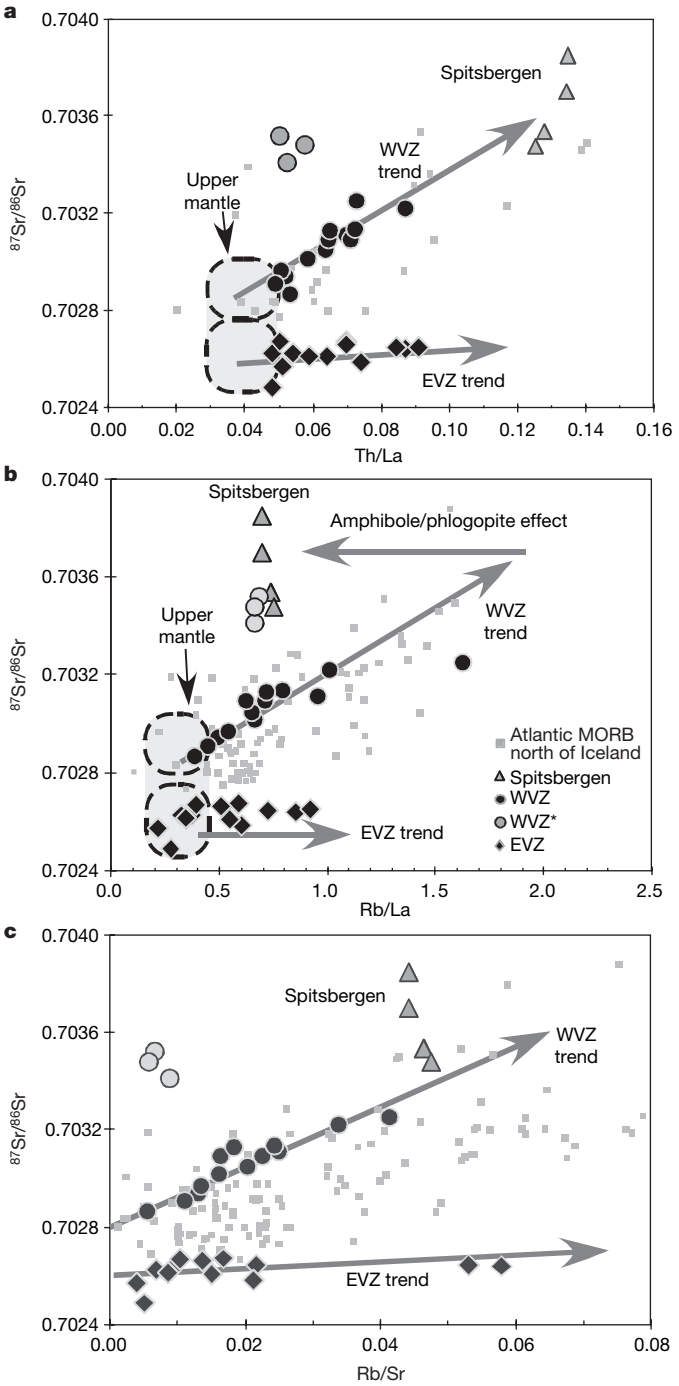

Figure 3 | Gakkel ridge and Spitsbergen basalts. a, $^{87}Sr/^{86}Sr$ versus Th/La. (The key is the same as that in **b**.) WVZ and EVZ lavas form distinct trends. WVZ data points display a trend towards those for Spitsbergen, indicating that the Spitsbergen magma source is the enriched WVZ endmember. **b**, $^{87}Sr/^{86}Sr$ versus Rb/La. WVZ and EVZ lavas display distinct trends. Spitsbergen lava data points lie away from the WVZ trend, with low Rb/La values (and Ba/La values, not shown), which is consistent with partial melting in the presence of residual amphibole and/or phlogopite, and indicates a SCLM source. **c**, $^{87}Sr/^{86}Sr$ versus Rb/Sr. (The key is the same as that in **b**.) The Sr isotope ratios are distinct for the WVZ and EVZ even when Rb/Sr = 0. In **a** and **b**, for low Th/La and Rb/La values corresponding to depleted mantle composition estimates[32,33] (labelled 'upper mantle'), the WVZ and EVZ Sr isotope ratios also are different. In all three panels, 'depleted' WVZ compositions are consistent with Atlantic MORBs from north of Iceland, but EVZ compositions are distinct. MORB data are taken from the Petrological Database of the Ocean Floor.

even far from hotspots[6,7], the WVZ is unique among North Atlantic MORB, with Dupal characteristics dominating along ~350 km of the spreading axis. Their occurrence in Arctic MORB shows that Dupal characteristics are not simply an attribute of the Indian–South Atlantic oceanic mantle, but reflect processes that are more general.

The small geographical scale and well-understood tectonic history of the Eurasian basin affords opportunities to explore how the Dupal signature is created. Quaternary alkaline basalts ranging from hawaiites to nephelinitic basanites in northwestern Spitsbergen have been attributed to low-degree melting of subcontinental lithospheric mantle (SCLM)[8–10], and form an enriched endmember for WVZ lavas in isotope plots (Figs 1a and 2). This relationship also holds for trace elements that are highly incompatible for melting of both anhydrous and metasomatized mantle mineral assemblages, where abundance ratios in lavas are almost the same as in the mantle source (shown for $^{87}Sr/^{86}Sr$ versus Th/La and U/La in Fig. 3a and Supplementary Fig. 4a, respectively). The trace elements and isotopes together strongly indicate that the component causing the Dupal-like characteristics is also the source of Spitsbergen alkaline basalts.

Insight into the mineral assemblage of the Spitsbergen magma source can be gleaned from the comparison of elements more compatible in amphibole or phlogopite (such as Rb, Ba and K) with other elements unaffected by amphibole or phlogopite (such as Th, U and La). In plots of $^{87}Sr/^{86}Sr$ versus Rb/La (Fig. 3b) and Ba/Th (Supplementary Fig. 4b), Spitsbergen lavas deviate from the WVZ trend at low values of Rb/La and Ba/Th , respectively; however, they are not offset in plots involving Th, U and La. Such chemical behaviour indicates the presence of amphibole or phlogopite among the residual minerals[11,12]. Spitsbergen lavas include olivine, titanaugite and plagioclase, but no amphibole or phlogopite[8]. Because these phases are unstable at asthenospheric temperatures[12,13], the data require an SCLM source for Spitsbergen lavas. Subsequent asthenospheric melting beneath the Gakkel ridge would then release the Rb and Ba, leading to the relative enrichments of these elements in the lavas of the WVZ.

The data offer insight into the long-term history of the Gakkel asthenosphere. A Rb–Sr 'pseudo-isochron' plot (Fig. 3c) shows that the WVZ mantle least contaminated by SCLM is distinct from the EVZ mantle, because their respective $^{87}Sr/^{86}Sr$ values differ when Rb/Sr = 0. This WVZ–EVZ offset is further confirmed by comparing isotopes and trace elements (Fig. 3a, b and Supplementary Fig. 4). The 'least contaminated' WVZ lavas are similar to Atlantic MORB north of Iceland, in terms of Nd–Sr isotopes and combined isotopes and trace elements (Figs 1 and 3 and Supplementary Fig. 4), whereas the EVZ basalts are distinct from both groups. These observations suggest that WVZ isotopic relationships can be explained by the addition of Spitsbergen SCLM to the North Atlantic asthenosphere, and that the WVZ and EVZ are distinct mantle provinces. The Gakkel SMZ thus bounds distinct upper-mantle regions that have experienced long-term convective isolation.

The introduction of the Svalbard SCLM to the WVZ asthenosphere, the leakage of North Atlantic mantle into the Arctic, and the formation of the boundary can be understood in the context of Arctic tectonic history (Fig. 4). The Eurasian and Atlantic oceans were separated by continent when seafloor spreading began in the Arctic and North Atlantic 55–60 million years (Myr) ago[14]. During the early Oligocene epoch ~34 Myr ago, Greenland and Norway–Svalbard began to separate, accompanied by northwards propagation of North Atlantic ridges, with linkage of the Arctic and North Atlantic occurring ~10 Myr ago. Our data suggest that North Atlantic mantle flowed into the Arctic, accompanied by delamination and dispersal of the Svalbard SCLM. Whether this was simply a consequence of rifting or was facilitated by thermal erosion caused by an Arctic hotspot is beyond the scope of this work (a hotspot has been postulated to be responsible for the Yermak plateau (Fig. 4c), but its existence is disputed[15]). In any case, the Gakkel SMZ appears to be the surface

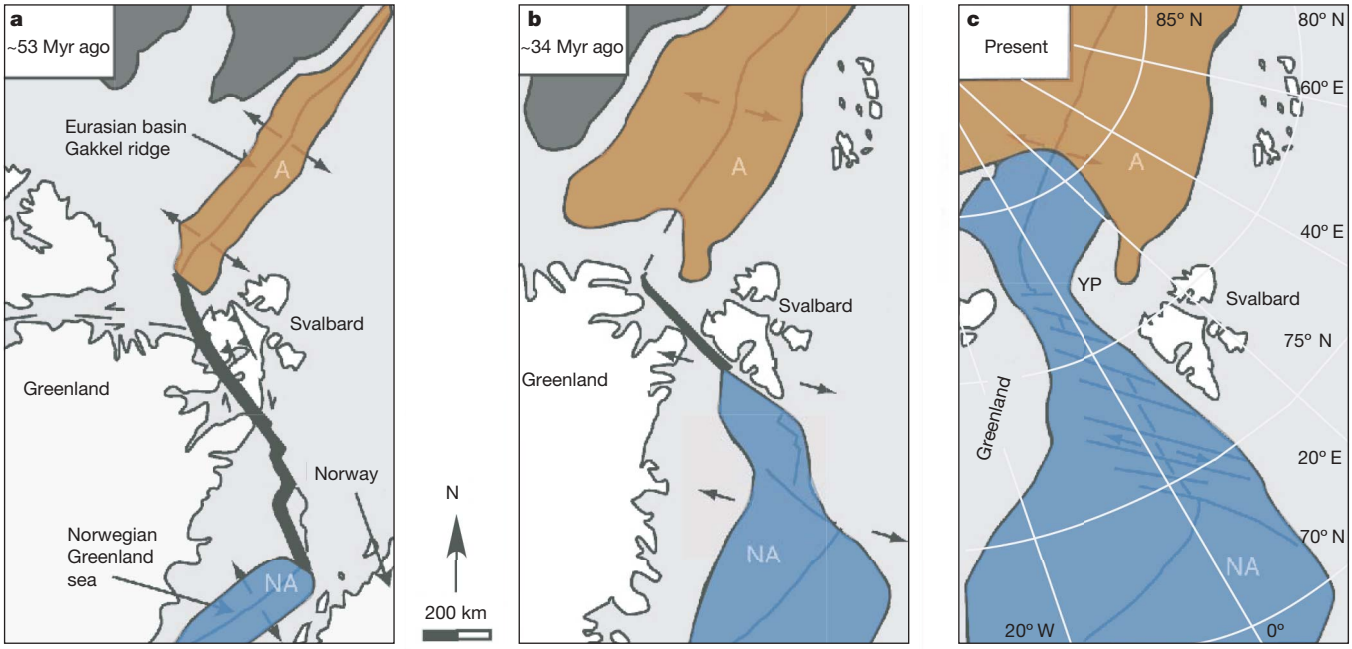

Figure 4 | Cenozoic-era evolution of the Arctic upper mantle. **a**, Approximately 53 Myr ago, the nascent Eurasian basin, underlain by 'Arctic' upper mantle (labelled 'A') as sampled today in the EVZ, was separated from the North Atlantic ridges (labelled 'NA') by a continent. **b**, During the Cenozoic, the Eurasian basin continued to widen, and the North Atlantic ridges propagated north, with Greenland and Svalbard separating ~10 Myr ago. **c**, Present-day situation based on the Gakkel data, with the boundary between the North Atlantic and Arctic upper-mantle provinces well within the Eurasian basin, in the middle of the SMZ. 'YP' labels the Yermak plateau, near the WVZ. Images modified from Blythe and Kleinspehn[14].

manifestation of a physical boundary within the mantle where the linkage occurred.

The origin of the Southern Hemisphere Dupal signature is an ongoing debate in mantle dynamics, and a recent summary highlights inadequacies of postulated models[16]. Explanations[16–28] include upwelling of a thermal anomaly from the core–mantle boundary; contamination of sub-Indian mantle by the Kerguelen plume; mantle modification by subduction surrounding Gondwana; ancient subduction of altered oceanic crust and sediment; recycled lower-continental or arc crust; and detachment of SCLM during continental break-up. Hybrid scenarios invoke both subduction and lithosphere delamination[29–31]. It has been suggested that SCLM delamination would impart 'too low' an osmium isotope signature to MORB[26,27], but this depends on the age of the recycled SCLM. The combined Gakkel and Spitsbergen data and the well-constrained Arctic tectonic history provide relationships where the geochemistry and tectonics are in remarkable accord.

In summary, the Gakkel ridge is an ultraslow-spreading ridge surrounded by continental lithosphere, with clear evidence of regional SCLM contributing a Dupal geochemical signature to the asthenospheric mantle. Unlike in other regions on Earth, we have the strong evidence of Spitsbergen volcanics, with the requisite isotopic compositions to be the Gakkel endmember, and a source mineralogy definitively indicating SCLM melting. The process documented in the Arctic is chemically and geologically feasible and probably plays an important role in generating chemical heterogeneity along the mid-ocean ridge system. Dupal signatures globally may have multiple sources; nevertheless, the migrating continents that have traversed the Indian Ocean basin, where Dupal characteristics occur on a large scale, would generate substantial opportunities for analogous SCLM contributions to the sub-Indian Ocean mantle.

METHODS SUMMARY

All analyses were made on hand-picked basaltic glasses. Major elements were measured on a Cameca electron microprobe at the American Museum of Natural History, operated as a joint facility with the Lamont-Doherty Earth Observatory of Columbia University (LDEO). Trace elements were measured using a Plasma Quad 2 inductively coupled plasma mass spectrometer at LDEO or a Thermo Electron X-series inductively coupled plasma mass spectrometer at Harvard. Pb, Nd and Sr isotope ratios were measured using a VG Sector 54 multicollector thermal ionization mass spectrometer at LDEO.

Full Methods and any associated references are available in the online version of the paper at www.nature.com/nature.

Received 15 January; accepted 14 March 2008.

1. Michael, P. J. *et al.* Magmatic and amagmatic seafloor generation at the ultraslow-spreading Gakkel ridge, Arctic Ocean. *Nature* **423,** 956–961 (2003).
2. Hart, S. R. A large-scale isotopic anomaly in the Southern Hemisphere mantle. *Nature* **309,** 753–757 (1984).
3. Mühe, R., Bohrmann, H., Garbe-Schönberg, D. & Kassens, H. E-MORB glasses from the Gakkel Ridge (Arctic Ocean) at 87°N: evidence for the Earth's most northerly volcanic activity. *Earth Planet. Sci. Lett.* **152,** 1–9 (1997).
4. Dick, H. J. B., Lin, J. & Schouten, H. An ultraslow-spreading class of ocean ridge. *Nature* **426,** 405–412 (2003).
5. Klein, E. M., Langmuir, C. H., Zindler, A., Staudigal, H. & Hamelin, B. Isotope evidence of a mantle convection boundary at the Australian-Antarctic Discordance. *Nature* **333,** 623–629 (1988).
6. Dosso, L. *et al.* The age and distribution of mantle heterogeneity along the Mid-Atlantic Ridge (31–41°N). *Earth Planet. Sci. Lett.* **170,** 269–286 (1999).
7. Shirey, S. B., Bender, J. F. & Langmuir, C. H. Three-component isotopic heterogeneity near the Oceanographer transform, Mid-Atlantic Ridge. *Nature* **325,** 217–223 (1987).
8. Skjelkvale, B. L., Amundsen, H. E. F., Oreilly, S. Y., Griffin, W. L. & Gjelsvik, T. A primitive alkali basaltic stratovolcano and associated eruptive centers, Northwestern Spitsbergen: Volcanology and tectonic significance. *J. Volcanol. Geotherm. Res.* **37,** 1–19 (1989).
9. Ionov, D. A., Bodinier, J. L., Mukasa, S. B. & Zanetti, A. Mechanisms and sources of mantle metasomatism: Major and trace element compositions of peridotite xenoliths from Spitsbergen in the context of numerical modeling. *J. Petrol.* **43,** 2219–2259 (2002).
10. Ionov, D. A., Mukasa, S. B. & Bodinier, J. L. Sr-Nd-Pb isotopic compositions of peridotite xenoliths from Spitsbergen: Numerical modelling indicates Sr-Nd decoupling in the mantle by melt percolation metasomatism. *J. Petrol.* **43,** 2261–2278 (2002).
11. Clague, D. A. & Frey, F. A. Petrology and trace element chemistry of the Honolulu volcanics, Oahu: Implication for the oceanic mantle below Hawaii. *J. Petrol.* **23,** 447–504 (1982).

12. Class, C. & Goldstein, S. L. Plume-lithosphere interactions in the ocean basins: constraints from the source mineralogy. *Earth Planet. Sci. Lett.* **150,** 245–260 (1997).
13. Niida, K. & Green, D. H. Stability and chemical composition of pargasitic amphibole in MORB pyrolite under upper mantle conditions. *Contrib. Mineral. Petrol.* **135,** 18–40 (1999).
14. Blythe, A. E. & Kleinspehn, K. L. Tectonically versus climatically driven exhumation of the Eurasian plate margin, Svalbard: Fission track analyses. *Tectonics* **17,** 621–639 (1998).
15. Ritzmann, O. & Jokat, W. Crustal structure of northwestern Svalbard and the adjacent Yermak Plateau: evidence for Oligocene detachment tectonics and non-volcanic breakup. *Geophys. J. Int.* **152,** 139–159 (2003).
16. Zhang, S. Q. *et al.* Evidence for a widespread Tethyan upper mantle with Indian-Ocean-type isotopic characteristics. *J. Petrol.* **46,** 829–858 (2005).
17. Dupré, B. & Allègre, C. J. Pb–Sr isotope variation in Indian Ocean basalts and mixing phenomena. *Nature* **303,** 142–146 (1983).
18. Hawkesworth, C. J., Mantovani, M. S. M., Taylor, P. N. & Palacz, Z. Evidence from the Paraña of south Brazil for a continental contribution to Dupal basalts. *Nature* **322,** 356–359 (1986).
19. Castillo, P. The Dupal anomaly as a trace of the upwelling lower mantle. *Nature* **336,** 667–670 (1988).
20. Arndt, N. T. & Goldstein, S. L. An open boundary between lower continental crust and mantle: its role in crust formation and crustal recycling. *Tectonophysics* **161,** 201–212 (1989).
21. le Roex, A. P., Dick, H. J. B. & Fisher, R. L. Petrology and geochemistry of MORB from 25°E to 46°E along the Southwest Indian Ridge: Evidence for contrasting styles of mantle enrichment. *J. Petrol.* **30,** 947–986 (1989).
22. Mahoney, J. J. *et al.* Isotopic and geochemical provinces of the Western Indian Ocean spreading centers. *J. Geophys. Res.* **94,** 4033–4052 (1989).
23. Barling, J., Goldstein, S. L. & Nicholls, I. A. Geochemistry of Heard Island (southern Indian Ocean): Characterization of an enriched mantle component and implications for the enrichment of the sub-Indian Ocean mantle. *J. Petrol.* **35,** 1017–1053 (1994).
24. Rehkamper, M. & Hofmann, A. W. Recycled ocean crust and sediment in Indian Ocean MORB. *Earth Planet. Sci. Lett.* **147,** 93–106 (1997).
25. Kempton, P. D. *et al.* Sr-Nd-Pb-Hf isotope results from ODP Leg 187: Evidence for mantle dynamics of the Australian-Antarctic Discordance and origin of the Indian MORB source. *Geochem. Geophys. Geosyst.* **3,** doi:10.1029/2002GC000320 (2002).
26. Hanan, B. B., Blichert-Toft, J., Pyle, D. G. & Christie, D. M. Contrasting origins of the upper mantle revealed by hafnium and lead isotopes from the Southeast Indian Ridge. *Nature* **432,** 91–94 (2004).
27. Escrig, S., Capmas, F., Dupré, B. & Allègre, C. J. Osmium isotopic constraints on the nature of the DUPAL anomaly from Indian mid-ocean-ridge basalts. *Nature* **431,** 59–63 (2004).
28. Meyzen, C. M. *et al.* New insights into the origin and distribution of the DUPAL isotope anomaly in the Indian Ocean mantle from MORB of the Southwest Indian Ridge. *Geochem. Geophys. Geosyst.* **6,** doi:10.1029/2005GC000979 (2005).
29. Geldmacher, J., Hoernle, K., Klugel, A., van den Bogaard, P. & Bindemann, I. Geochemistry of a new enriched mantle type locality in the northern hemisphere: Implications for the origin of the EM-I source. *Earth Planet. Sci. Lett.* **265,** 167–182 (2008).
30. le Roux, P. J. *et al.* Mantle heterogeneity beneath the southern Mid-Atlantic Ridge: trace element evidence for contamination of ambient asthenospheric mantle. *Earth Planet. Sci. Lett.* **203,** 479–498 (2002).
31. Janney, P. E., le Roex, A. P. & Carlson, R. W. Hafnium isotope and trace element constraints on the nature of mantle heterogeneity beneath the central Southwest Indian Ridge (13°E to 47°E). *J. Petrol.* **46,** 2427–2464 (2005).
32. Salters, V. J. M. & Stracke, A. Composition of the depleted mantle. *Geochem. Geophys. Geosyst.* **5,** doi:10.1029/2003GC000597 (2004).
33. Workman, R. K. & Hart, S. R. Major and trace element composition of the depleted MORB mantle (DMM). *Earth Planet. Sci. Lett.* **231,** 53–72 (2005).

Supplementary Information is linked to the online version of the paper at www.nature.com/nature.

Acknowledgements We thank A. le Roex for comments that helped to improve this paper. This work was supported by the US National Science Foundation. G.S. was supported partly by a Paul and Daisy Soros Fellowship for New Americans.

Author Information The geochemical data reported here are available in the Petrological Database of the Ocean Floor (www.petdb.org). Reprints and permissions information is available at www.nature.com/reprints. Correspondence and requests for materials should be addressed to S.L.G. (steveg@ldeo.columbia.edu).

METHODS

Major elements. Major elements were measured at the American Museum of Natural History on the AMNH-LDEO Cameca electron microprobe. Each analysis represents an average of five individual measurements on a single glass chip. A glass chip of the Lamont glass probe standard, JDF-D2, was repeatedly analysed in each probe session to monitor long-term drift. No long-term drift was evident in any run. The errors are based on the reproducibility of JDF analyses over multiple probe sessions and are $\leq$1% for SiO_2 and MgO.

Trace elements. Hand-picked glass separates with minimal surface alteration were analysed for trace element compositions and measured on the Plasma Quad 2 inductively coupled plasma mass spectrometer at LDEO or a Thermo Electron X-series inductively coupled plasma mass spectrometer at Harvard . Solutions were spiked with Ge, In, Tm and Bi to correct for in-run drift. Concentrations were determined using a calibration curve based on US Geological Survey and in-house standards measured during each run. Errors are 3–5%.

Isotope ratios. Pb, Nd and Sr isotope ratios were measured on separate glass chips from the trace element analyses. These were leached cold for 12 minutes with 8N HNO_3. Pb was separated using AG1-X8 anion resin, Sr was separated using Eichrom Sr resin and Nd was separated in a two-column procedure using Eichrom TRU-spec resin to separate the rare-earth elements, followed by α-hydroxy isobutyric acid. Sr, Nd and Pb isotopes were measured on a VG Sector 54 multicollector thermal ionization mass spectrometer at LDEO. $^{87}Sr/^{86}Sr$ ratios were normalized to $^{86}Sr/^{88}Sr = 0.1194$. Sr isotopes were measured in multidynamic mode. Instrumental reproducibility was monitored by repeated measurements of the US National Institute of Standards and Technology SRM 987 standard, which yielded $^{87}Sr/^{86}Sr = 0.710246 \pm 0.000016$ (2-s.d. external reproducibility, $n > 40$). All samples were further corrected to a value of 0.71024 for SRM 987. All Nd analyses were made in multidynamic mode as NdO^+. $^{143}Nd/^{144}Nd$ ratios were normalized to $^{146}Nd/^{144}Nd = 0.7129$. Repeated measurements of the La Jolla Nd standard yielded $^{143}Nd/^{144}Nd = 0.511838 \pm 0.000012$ (2-s.d. external reproducibility, $n > 30$). All samples were further corrected to a value of 0.511860 for the La Jolla standard. Pb isotope analyses used a ^{207}Pb–^{204}Pb double spike. All measurements were performed in static mode. Measurements of unspiked–double-spiked pairs of the NBS 981 standard were replicated to 183, 284 and 300 p.p.m. (2-s.d. external reproducibility, $n = 20$) for $^{206}Pb/^{204}Pb$, $^{207}Pb/^{204}Pb$ and $^{208}Pb/^{204}Pb$ ratios, respectively. These measured Pb isotope ratios were corrected to the Todt *et al.*[34] values of 16.9356, 15.4891, and 36.7006, respectively, for NBS 981.

34. Todt, W., Cliff, R. A., Hanser, A. & Hofmann, A. W. in *Earth Processes: Reading the Isotopic Code* Vol. 95 (eds Basu, A. & Hart, S. R.) 429–437 (American Geophysical Union, Washington DC, 1996).

SUPPLEMENTARY INFORMATION

Supplementary Information for "Origin of a 'Southern Hemisphere' geochemical signature in the Arctic upper mantle" by S.L. Goldstein, G. Soffer, C.H. Langmuir, K.A. Lehnert, D.W. Graham, and P.J. Michael.

Section S1 includes Data Tables.

Table S1. Locations of analyzed Gakkel Ridge axial basalts
Table S2. Sr, Nd, Pb isotope data on Gakkel Ridge basalts
Table S3. Chemical data on Gakkel Ridge basalts

Section S2 includes additional discussion, with 4 figures.

Section S1: Gakkel Ridge Axial Basalt Data

Table S1. Locations of analyzed Gakkel Ridge axial basalts

Sample ID	Latitude	Longitude**	Depth (mbsl)	Distance*
WVZ				
H-011-026	83.01	-6.34	-3996	11
H-008-011	82.90	-6.24	-4042	23
P-216-010	83.08	-6.07	-3570	24
H-012-017	83.01	-4.98	-3007	34
H-R005	83.50	-4.49	-1888	46
H-021-004	83.86	-1.94	-3076	107
H-R007	83.88	-1.77	-1432	110
H-023-026	84.01	-0.47	-3485	130
H-006-001	84.13	0.52	-3618	151
H-R002	84.12	0.57	-1740	152
H-025-005	84.39	2.11	-3698	187
H-026-020	84.46	2.57	-4169	197
H-027-029	84.48	2.78	-4033	200
WVZ*				
H-005-001	84.44	2.12	-4099	192
H-005-002	84.44	2.12	-4099	192
H-028-015	84.50	2.66	-4075	201
West-SMZ				
H-036-001	85.26	12.41	-4411	338
H-038-029	85.31	12.69	-4676	345
H-038-025	85.31	12.69	-4676	345
East-SMZ				
H-R001	85.56	15.98	-2397	386
P-199-1-007-04	85.57	16.17	-4666	388
P-199-1-001-03	85.57	16.17	-4666	388
H-041-017	85.69	17.90	-3982	409
P-318-098-B (A-M)	85.88	22.30	-4832	447
P-312-011	85.91	27.30	-4123	489
EVZ				
H-R012	86.06	32.61	-2046	534
H-094-003	86.08	33.16	-4398	538
H-050-044	86.34	36.94	-3776	575
P-307-SG1	86.34	38.14	-4743	582
H-052-008	86.52	42.14	-3822	612
H-082-005	86.61	44.75	-4890	630

H-078-004	86.83	51.72	-5070	671
H-073-012	86.96	57.36	-4037	699
H-057-046	86.56	67.54	-2787	741
H-058-002	86.53	70.00	-3103	751
H-067-001	86.40	72.68	-1977	764
H-063-004	85.63	84.58	-3939	840
H-061-003	85.63	85.05	-3870	842

Table S1 caption: The listed sample ID is an abbreviation for the official names. H refers to samples collected by the USCGC Healy. The official format for dredges is H-X-Y where H=H0102, X=site/dredge number, Y=sample number within dredge; and for rock cores is H-RZZZ, where H=H0102, R=rock core, and Z is the rock core number. P refers to samples collected by the FS Polarstern, where the official format is P-X-Y where P=POL0059, X=site number, and Y=sample name. Latitude and Longitude are given in decimal degrees. **Minus for longitude means west of the Greenwich meridian. Depth is rock core depth or average dredge depth in meters below sea level (mbsl). *Distance refers to distance along the ridge axis from the intersection of the Gakkel Ridge and the Lena Trough, near Greenland.

Table S2. Sr, Nd, Pb isotope data on Gakkel Ridge basalts

Sample ID	$^{87}Sr/^{86}Sr$	$^{143}Nd/^{144}Nd$	$^{206}Pb/^{204}Pb$	$^{207}Pb/^{204}Pb$	$^{208}Pb/^{204}Pb$	Δ7/4	Δ8/4	ΔSr
WVZ								
H-011-026	0.703255	0.513043	17.9703	15.4273	37.7317	-1.17	37.9	32.6
H-008-011	0.703114	0.513103	18.0049	15.4269	37.7815	-1.58	38.7	31.1
P-216-010	0.703020	0.513101	18.0623	15.4360	37.8153	-1.29	35.1	30.2
H-012-017	0.703098	0.513079	18.0944	15.4389	37.8846	-1.35	38.2	31.0
H-R005	0.703223	0.513066	17.9920	15.4283	37.8662	-1.31	48.7	32.2
H-021-004	0.703051	0.513095	18.0474	15.4331	37.8262	-1.43	38.0	30.5
H-R007	0.703093	0.513100	18.0276	15.4246	37.7872	-2.06	36.5	30.9
H-023-026	0.703139	0.513067	18.0298	15.4328	37.8628	-1.26	43.8	31.4
H-006-001	0.702944	0.513128	18.0743	15.4353	37.7936	-1.50	31.5	29.4
H-R002	0.702970	0.513112	18.1005	15.4380	37.8345	-1.51	32.4	29.7
H-025-005	0.703131	0.513051	18.0754	15.4329	37.8358	-1.75	35.6	31.3
H-026-020	0.702911	0.513104	18.0704	15.4330	37.7798	-1.68	30.6	29.1
H-027-029	0.702868	0.513123	18.0965	15.4355	37.7779	-1.72	27.2	28.7
WVZ*								
H-005-001	0.703411	0.513028	18.0518	15.4356	37.8270	-1.22	37.5	34.1
H-005-002	0.703521	0.513011	18.0607	15.4391	37.8547	-0.96	39.2	35.2
H-028-015	0.703481	0.513025	18.1280	15.4429	37.9250	-1.32	38.1	34.8
West-SMZ								
H-036-001	0.703411	0.513054	17.6799	15.3899	37.5477	-1.76	54.6	34.1
H-038-029	0.702998	0.513149	18.0607	15.4391	37.8547	-0.96	39.2	30.0
H-038-025	0.703021	0.513120						30.2
West-SMZ								
H-R001	0.702909	0.512990	18.8144	15.5446	38.4277	1.41	5.4	29.1
P-199-1-007-04	0.702699	0.513125	18.1929	15.4534	37.8563	-0.97	23.4	27.0
P-199-1-001-03	0.702763	0.513076	18.6081	15.5168	38.2370	0.87	11.3	27.6
H-041-017	0.702820							28.2
P-318-098-B (A-M)	0.702550	0.513224	17.9799	15.4335	37.6212	-0.65	25.7	25.5
P-312-011	0.702632	0.513222	17.8299	15.4282	37.4541	0.44	27.1	26.3
EVZ								
H-R012	0.702641	0.513236	17.8900	15.4352	37.4987	0.49	24.3	26.4
H-094-003	0.702648	0.513238	17.9032	15.4417	37.5159	1.00	24.4	26.5
H-050-044	0.702647	0.513179	18.0554	15.4400	37.6606	-0.82	20.5	26.5
P-307-SG1	0.702586	0.513214	17.9968	15.4288	37.6012	-1.30	21.6	25.9

H-052-008	0.702673	0.513162	18.0840	15.4350	37.6772	-1.63	18.7	26.7
H-082-005	0.702611	0.513202	17.9571	15.4264	37.5557	-1.11	21.9	26.1
H-078-004	0.702627	0.513175	17.9953	15.4327	37.6067	-0.90	22.3	26.3
H-073-012	0.702627	0.513162	18.0492	15.4438	37.6704	-0.37	22.2	26.3
H-057-046	0.702671	0.513151	18.0703	15.4436	37.6603	-0.63	18.6	26.7
H-058-002	0.702664	0.513128	18.0547	15.4362	37.6594	-1.20	20.4	26.6
H-067-001	0.702488	0.513193	17.9752	15.4231	37.5858	-1.64	22.7	24.9
H-063-004	0.702613	0.513132	17.9844	15.4348	37.5994	-0.57	22.9	26.1
H-061-003	0.702572	0.513153	17.9880	15.4308	37.5836	-1.01	20.9	25.7

Table S2 caption: Details of analytical methods and errors are given in the Methods section. $\Delta 7/4$, $\Delta 8/4$, and ΔSr are defined by Hart[1] and reflect the deviation of sample $^{207}Pb/^{204}Pb$, $^{208}Pb/^{204}Pb$, and $^{87}Sr/^{86}Sr$ ratios from the Northern Hemisphere Reference Line (NHRL), reflecting typical values of Northern Hemisphere basalts.

Table S3. Chemical data on Gakkel Ridge basalts

Sample ID	MgO	SiO_2	K_2O	Ba	Rb	Th	U	La	Sr	Nd
WVZ										
H-011-026	7.74	50.14	0.339	73.6	7.15	0.320	0.088	4.41	174	10.9
H-008-011	7.92	50.83	0.214	45.7	3.70	0.270	0.070	3.89	149	11.0
P-216-010	7.83	50.43	0.17	31.3	2.45	0.217	0.064	3.72	152	10.5
H-012-017	7.21	50.36	0.267	48.6	3.66	0.369	0.097	5.21	164	12.8
H-R005	6.02	51.24	0.266	85.0	5.61	0.484	0.117	5.57	166	12.1
H-021-004	6.53	50.98	0.242	41.4	3.23	0.316	0.090	5.00	159	12.6
H-R007	8.06	50.5	0.167	23.1	2.31	0.239	0.066	3.72	142	10.2
H-023-026	7.59	50.61	0.23	49.3	3.70	0.340	0.088	4.71	152	12.0
H-006-001	7.85	49.99	0.157	26.5	1.89	0.200	0.064	3.88	146	11.5
H-R002	7.62	50.2	0.146	23.8	1.96	0.185	0.050	3.66	148	11.1
H-025-005	7.89	49.7	0.215	36.6	2.87	0.260	0.080	4.03	158	11.2
H-026-020	8.21	49.53	0.127	21.5	1.65	0.180	0.050	3.71	150	11.2
H-027-029	9.06	48.91	0.069	6.9	0.57	0.080	0.019	1.51	106	6.05
WVZ*										
H-005-001	7.69	48.23	0.133	24.0	1.89	0.150	0.050	2.87	217	10.5
H-005-002	7.60	46.69	0.097	18.7	1.50	0.110	0.030	2.21	227	9.90
H-028-015	8.67	46.81	0.089	18.3	1.27	0.110	0.040	1.92	226	8.35
West-SMZ										
H-036-001	6.80	52.05	0.742	249.0	23.80	1.490	0.360	11.70	212	15.1
H-038-029	7.60	50.57	0.319	93.4	7.92	0.590	0.160	6.21	168	11.4
H-038-025	7.21	50.72	0.354	98.4	8.84	0.647	0.179	6.72	163	12.3
West-SMZ										
H-R001	9.39	47.55	0.103	11.9	1.00	0.162	0.066	3.32	194	7.77
P-199-1-007-04	8.90	49.11	0.136	31.0	2.66	0.251	0.072	3.16	137	8.05
P-199-1-001-03	8.50	48.07	0.049	8.1	0.68	0.083	0.027	1.86	138	6.37
H-041-017	8.10	50.67	0.266	69.3	5.62	0.410	0.120	4.98	193	9.56
P-318-098-B (A-M)	5.72	51.7	0.555	133.1	10.96	1.110	0.326	10.91	149	21.1
P-312-011	7.33	50.54	0.401							
EVZ										
H-R012	4.51	50.94	0.72	124.1	8.44	0.864	0.278	9.91	146	19.1
H-094-003	5.63	50.51	0.501	109.1	8.23	0.814	0.385	8.97	155	16.5
H-050-044	8.21	49.61	0.365	61.0	4.54	0.530	0.160	6.27	210	11.6
P-307-SG1	7.53	50.24	0.269	47.7	3.68	0.451	0.142	6.09	173	12.8
H-052-008	7.75	50.91	0.303	82.9	3.58	0.425	0.175	6.10	212	11.8

H-082-005	7.95	50.31	0.257	36.5	2.95	0.345	0.114	5.38	194	11.4
H-078-004	8.70	49.87	0.171	20.9	1.54	0.226	0.082	4.17	171	9.74
H-073-012	8.53	49.94	0.176	17.8	1.34	0.200	0.092	4.17	198	9.82
H-057-046	8.12	49.18	0.256	23.7	2.13	0.274	0.121	5.43	206	12.7
H-058-002	7.95	49.73	0.28	35.8	2.70	0.371	0.122	5.32	198	11.3
H-067-001	8.49	49.97	0.123	12.3	0.90	0.159	0.050	3.31	173	9.60
H-063-004	8.22	49.94	0.274	24.8	1.85	0.319	0.120	5.41	216	11.4
H-061-003	8.76	49.53	0.168	13.6	0.86	0.204	0.065	3.98	216	10.9

Table S3 caption: Details of analytical methods and errors are given in the Methods section.

Section S3: Additional Discussion

This section provides further elaboration on some of the points discussed in the main text. The subjects addressed are: (1) the abrupt isotopic boundary in the Gakkel "sparsely magmatic zone" (SMZ); (2) the isotopic characteristics that distinguish the Gakkel western volcanic zone (WVZ) from the Gakkel eastern volcanic zone (EVZ), the adjacent Knipovich and Mohns Ridges to the south, other enriched North Atlantic MORB from the Oceanographer Fracture Zone; (3) additional evidence beyond what is discussed in the main text that the WVZ shows a true DUPAL isotopic signature; (4) additional evidence beyond what is discussed in the main text, that Spitsbergen Quaternary alkaline basalts are derived from melting in the presence of residual amphibole or phlogopite, thus reflect melting of the subcontinental lithospheric mantle (SCLM), and that this SCLM is also the source of the DUPAL geochemical signal in the western Gakkel Ridge.

The abrupt isotopic boundary in the SMZ: Figure 1a in the main text shows that Nd-Sr isotope ratios of Gakkel Ridge basalts from east and west of the isotopic boundary in the SMZ plot in distinct fields, and Figure 1b shows that the boundary is abrupt using $\Delta 8/4$ of Hart[1]. However, $\Delta 8/4$ is not strictly an analytical measurement, as it reflects the deviation from the Northern Hemisphere Reference Line of Hart[1], and thus has a strong interpretive quality. Figure S1 shows that the EVZ and WVZ are distinct using isotope ratios, in this case $^{87}Sr/^{86}Sr$. It also shows that the isotopes must be interpreted in combination. While Sr isotope ratios of samples near the isotopic boundary are similar, the combined Nd-Sr isotope ratios of these samples (shown in Figure 1 of the main text) are distinct.

Comparisons with ridges to the south: The Gakkel WVZ compositions are not only distinct from the Gakkel EVZ basalts, they are also distinct from neighboring ridges to the south. Figure S1b is an additional along axis plot using another isotope ratio, in this case $^{206}Pb/^{204}Pb$, and includes published data from the neighboring Knipovich and Mohns Ridges to the south, offset

600 km from the WVZ by the Lena Trough. Pb isotope ratios of Knipovich and Mohns ridge lavas are overwhelmingly higher than those seen in the Gakkel Ridge.

Figure S2a,b extends this comparison, showing $^{208}Pb/^{204}Pb$ and $^{207}Pb/^{204}Pb$ vs $^{206}Pb/^{204}Pb$ ratios of Gakkel Ridge axial lavas and Spitsbergen alkaline basalts with the Knipovich and Mohns data, and the enriched ("A") group of samples from the Oceanographer Fracture Zone (OFZ) along the Mid-Atlantic Ridge, whose distinct compositions compared to neighboring samples were interpreted by Shirey et al.[2] to reflect contributions from delaminated SCLM. The Atlantic data display a large range of $^{206}Pb/^{204}Pb$ ratios, with Gakkel lavas at the lower end (seen also in Fig. S1b). Figure S2a shows that all of these North Atlantic data are offset from NHRL, at the same time the greater offset of Gakkel WVZ lavas compared to all the others, to higher $^{208}Pb/^{204}Pb$ for a given $^{206}Pb/^{204}Pb$, can be clearly seen. The OFZ lavas are on the trend shown by the Knipovich and Mohns compositions, and have little in common with the Gakkel WVZ.

The DUPAL signal in the western Gakkel Ridge: Characteristics of the western Gakkel basalts illustrated in the main text include high $\Delta 8/4 > 30$[1] (Fig. 1b), $^{208}Pb/^{204}Pb$ vs $^{206}Pb/^{204}Pb$ values that plot with Indian Ocean MORB and South Atlantic DUPAL MORB, but are distinct from Pacific and non-DUPAL Atlantic MORB (Fig. 2a), and a DUPAL trend in $^{206}Pb/^{204}Pb$ vs Sr isotopes, like Indian MORB and South Atlantic DUPAL MORB. Figure S2a further illustrates the distinctively high $^{208}Pb/^{204}Pb$ vs $^{206}Pb/^{204}Pb$ compared to eastern Gakkel basalts as well as the Knipovich and Mohns ridges, and the enriched group of lavas from the Oceanographer Fracture Zone. Figure S3a takes this comparison further using $\Delta 8/4$, quantifying the offset from NHRL for these samples, showing that western Gakkel lavas are distinct among these North Atlantic MORB. Figure S3b shows that western Gakkel lavas plot with Indian MORB and South Atlantic DUPAL MORB in $\Delta 8/4$ vs ΔSr.

We conclude that these data altogether show that the isotopic characteristics of western Gakkel MORB are clearly DUPAL in the sense that they show the primary isotopic characteristics of Southern Hemisphere DUPAL MORB. As discussed in the text, the western Gakkel Ridge is distinct from Indian MORB and South Atlantic DUPAL MORB, having low Δ7/4 and plotting near (or even below) NHRL (Fig. S2b). We posit that this reflects the timing of U/Pb fractionation, rather than the process that generates the DUPAL signature. In this context, recently published data by Geldmacher et al.[3] on two samples from the Godzilla Seamount in the eastern Atlantic near Madeira show strong EM1 characteristics (negative εNd and εHf of ~-4 and ~-6.5, respectively, high $^{87}Sr/^{86}Sr$ of ~0.7057, very high Δ8/4 values of >100, but low Δ7/4 values of about -7, thus below NHRL. They come to the same conclusion as we do that Δ7/4 reflects timing rather than process and thus should not be a criterion for labelling enriched mantle components.

Evidence that the source of Spitsbergen alkaline basalts is the SCLM, and also the source of the DUPAL geochemical signal in the western Gakkel Ridge. Evidence that the source of Quaternary Spitsbergen alkaline basalts is an end-member mixing component for Gakkel Ridge lavas is shown by isotope ratios and the combination of isotope and trace element ratios. Spitsbergen compositions are on extensions of WVZ compositions with in Nd-Sr isotope space (Fig. 1a), and in $^{206}Pb/^{204}Pb$-Sr isotope space (Fig. 2b). Moreover Spitsbergen lavas have the same offset from NHRL as Gakkel WVZ lavas in terms of $^{208}Pb/^{204}Pb$-$^{206}Pb/^{204}Pb$ (Figs. 2a, S2a). In addition, they have the same low Δ7/4 (Fig. S2b). In terms of trace element-isotope combinations, in the main text we show that Spitsbergen compositions lie on extensions of the WVZ trend in terms of both Th/La vs Sr isotopes (Fig. 3a), while the EVZ does not. Here we show that this is also the case with U/La vs Sr isotopes (Fig. S4a). Moreover, complementary relationships can be shown using Nd isotopes (not shown). Having established the linkage between the Spitsbergen and WVZ magma sources, we also confirm literature interpretions of the Spitsbergen lavas as small degree melts of the subcontinental lithospheric mantle[4-7] by

showing evidence for residual amphibole or phlogopite in the melting source. In this case, Th, U, La are highly incompatible elements, like they are in anhydrous mantle assemblages, while Rb, Ba, K are more compatible than in anhydrous mantle assemblages[8-10]. In the text we show that Spitsbergen lavas do not lie on the WVZ trend for Rb/La vs Sr isotopes (Fig. 3b), but have low Rb/La, consistent with melting in the presence of residual amphibole or phlogopite. Here we show in addition that Spitsbergen and WVZ lavas show the same relationships for Ba/Th vs Sr isotopes (Fig. S4b). The same relationships hold for K/La or K/Th (not shown). Altogether, these relationships strongly indicate melting the Spitsbergen magmas were generated in the presence of residual amphibole or phlogopite, whose presence strongly in the subcontinental lithospheric mantle (SCLM), because these phases are unstable at asthenospheric temperatures[11-13]. It follows from all of these considerations that the source of the DUPAL-like compositions in the western Gakkel mantle is Spitsbergen SCLM.

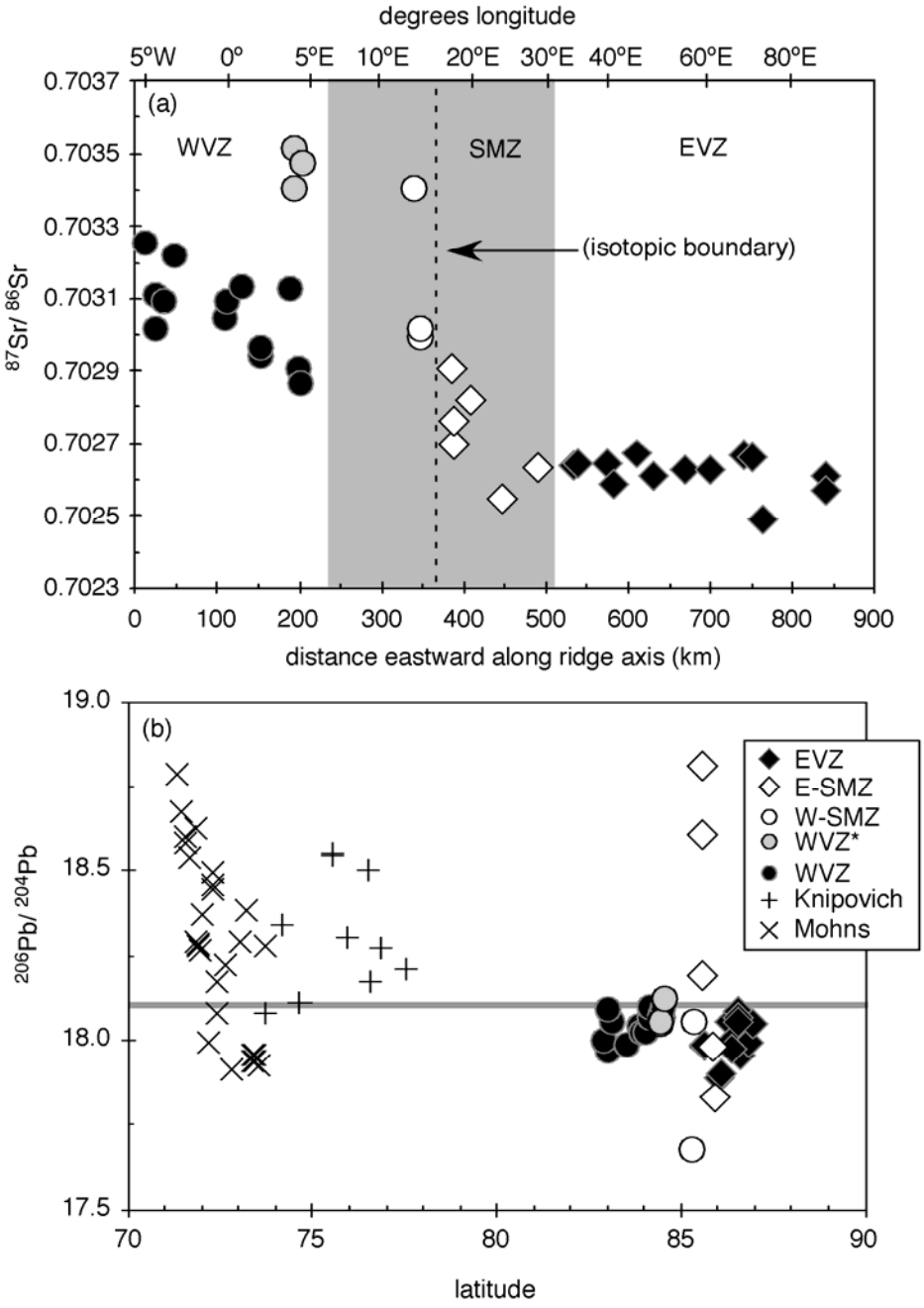

Figure S1. Along-axis chemical relationships in the Arctic and far North Atlantic. (a) Sr isotope ratios in Gakkel basalts vs distance from the Lena Trough near Greenland. The frame illustrates the distinctive WVZ and EVZ compositions and the position of the isotopic boundary. Although the Sr isotope ratios of the samples staddling the boundary in are similar, they are distinct in Nd-Sr space (Fig. 1*a*), with western and eastern SMZ samples plotting with the adjacent tectono-magmatic zones. (b) $^{206}Pb/^{204}Pb$ ratios vs latitude to include lavas from the Knipovich and Mohns Ridges to the south, showing that they are distinct from the Western Gakkel samples. Knipovich and Mohns Ridge data are from refs.[14-17].

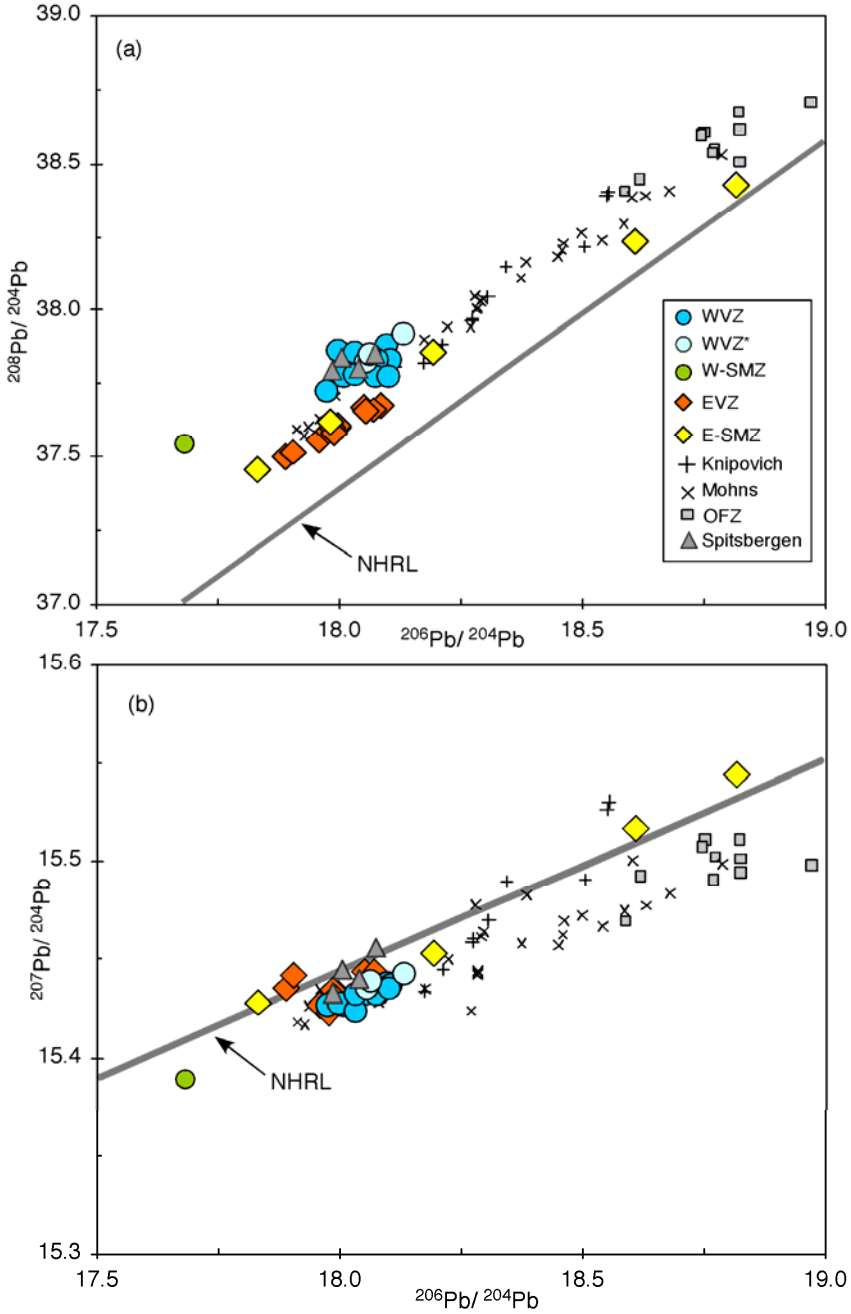

Figure. S2. Pb isotope relationships of Gakkel Ridge basalts, compared with far North Atlantic spreading ridges, enriched samples from the Oceanographer Fracture Zone (OFZ), and Spitsbergen alkaline lavas. In (a) $^{208}Pb/^{204}Pb$ vs $^{206}Pb/^{204}Pb$, all are offset to high $^{208}Pb/^{204}Pb$ compared L, but Gakkel WVZ and Spitsbergen lavas are offset to higher $^{208}Pb/^{204}Pb$ compared to all the others. In general, Knipovich and Mohns Ridge lavas have higher Pb isotope ratios than Gakkel lavas. Enriched OFZ lavas have the highest Pb isotope ratios and are similar in character to Knipovich and Mohns lavas. In (b) $^{207}Pb/^{204}Pb$ vs $^{206}Pb/^{204}Pb$, all fall on a similar trend, parallel to NHRL but below it. NHRL is from Hart[1], the OFZ lavas are from the "enriched A Group" of Shirey et al.[2]. Literature Pb isotope data are from refs.[2,6,14-17].

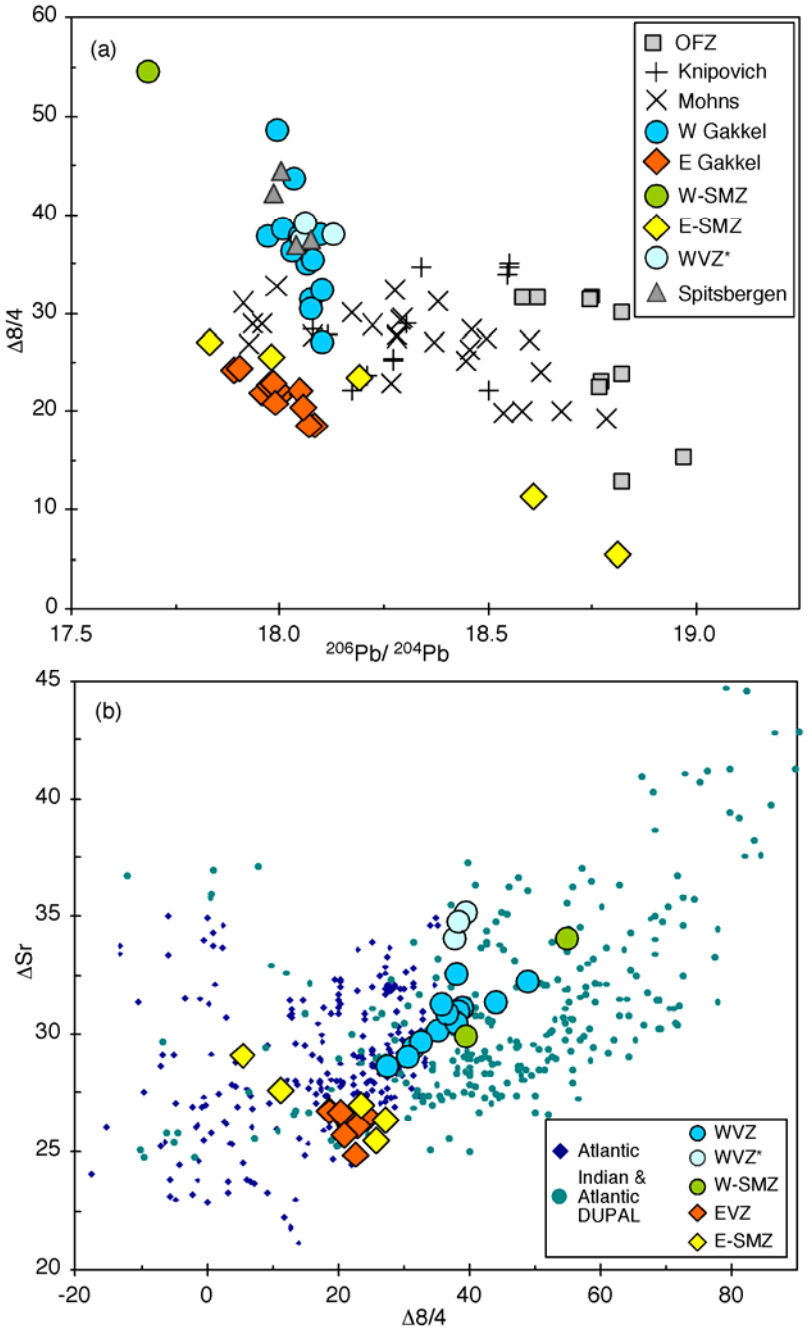

Figure S3. DUPAL parameters of Gakkel basalts. (a) Δ8/4 vs $^{206}Pb/^{204}Pb$ ratios compared with far North Atlantic spreading ridges, enriched samples from the Oceanographer Fracture Zone (OFZ), and Spitsbergen alkaline lavas. Most of the western Gakkel basalts have Δ8/4 values higher than all analyzed basalts from the Knipovich and Mohns ridges, and the OFZ. (b) in terms of DSr vs D8/4, western Gakkel basalts clearly fall into the range of Indian and Atlantic DUPAL values and outside of the range of Atlantic non-DUPAL basalts. Knipovich, Mohns, OFZ and Spitsbergen data are from are from refs.[2,6,14-17]. Global MORB data are from the PetDB Database[18] (www.petdb.org). Δ8/4 and ΔSr are defined by Hart[1].

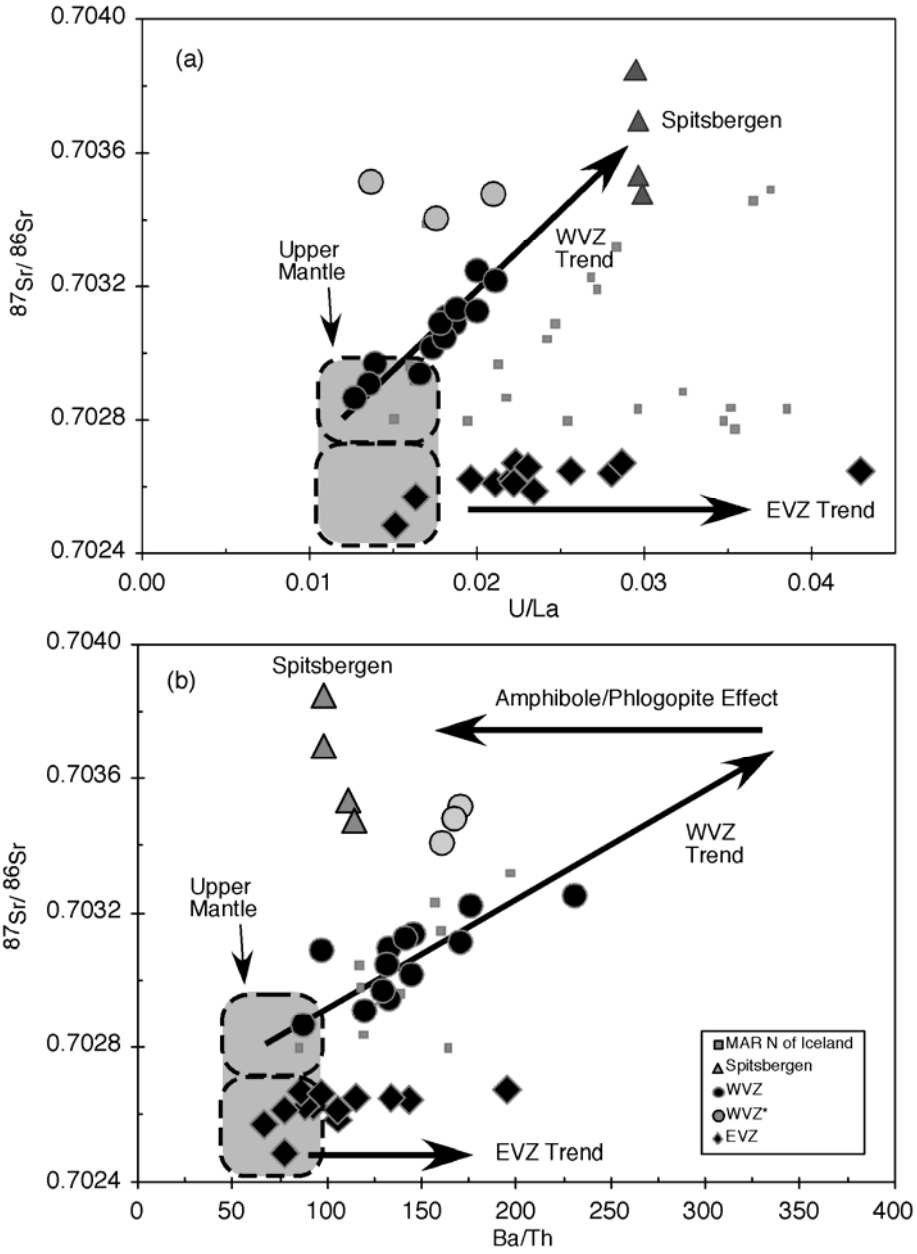

Figure S4. Spitsbergen, Gakkel, and SCLM. (a) U/La vs Sr isotopes show a trend for western Gakkel lavas toward the compositions of Quaternary alkaline lavas from Spitsbergen, like Th/La (main text Fig. 3a). Along with the isotopic evidence discussed in the main and supplementary text, this strongly indicates that the source of the Spitsbergen lavas is contributing to western Gakkel basalts. (b) Ba/Th in the Spitsbergen lavas are off the western Gakkel trend, with the low Ba/Th reflecting greater compatibility of Ba in the presence of residual amphibole or phlogopite, indicating melting of subcontinental lithospheric mantle. Both figures show that eastern and western Gakkel lavas have different Sr isotope ratios at U/La and Ba/La values appropriate to depleted upper mantle[19,20], showing that the "depleted" (low $^{87}Sr/^{86}Sr$, U/La, Ba/Th) mantle sources are different.

Supplementary References:

1 Hart, S.R. A large-scale isotopic anomaly in the Southern Hemisphere mantle. *Nature* **309** (5971), 753-757 (1984).

2 Shirey, S. B., Bender, J. F., & Langmuir, C. H. Three component isotopic heterogeneity near the Oceanographer Transform, Mid-Atlantic Ridge. *Nature* **325** (6101), 217-223 (1987).

3 Geldmacher, J., Hoernle, K., Klugel, A., van den Bogaard, P., & Bindemann, I. Geochemistry of a new enriched mantle type locality in the northern hemisphere: Implications for the origin of the EM-I source. *Earth and Planetary Science Letters* **265**, 167-182 (2008).

4 Skjelkvale, B.L., Amundsen, H.E.F., Oreilly, S.Y., Griffin, W.L., & Gjelsvik, T. A primitive alkali basaltic stratovolcano and associated eruptive centers, Northwestern Spitsbergen: Volcanology and tectonic significance. *Journal of Volcanology and Geothermal Research* **37** (1), 1-19 (1989).

5 Vagnes, E. & Amundsen, H.E.F. Late Cenozoic uplift and volcanism on Spitsbergen – caused by mantle convection. *Geology* **21** (3), 251-254 (1993).

6 Ionov, D.A., Mukasa, S.B., & Bodinier, J.L. Sr-Nd-Pb isotopic compositions of peridotite xenoliths from Spitsbergen: Numerical modelling indicates Sr-Nd decoupling in the mantle by melt percolation metasomatism. *Journal of Petrology* **43** (12), 2261-2278 (2002).

7 Ionov, D.A. , Bodinier, J.L., Mukasa, S.B., & Zanetti, A. Mechanisms and sources of mantle metasomatism: Major and trace element compositions of peridotite xenoliths from Spitsbergen in the context of numerical modeling. *Journal of Petrology* **43** (12), 2219-2259 (2002).

8 Adam, J., Green, T.H., & Sie, S.H. Proton Microprobe Determined Partitioning of Rb, Sr, Ba, Y, Zr, Nb and Ta between Experimentally Produced Amphiboles and Silicate Melts with Variable F Content. *Chemical Geology* **109** (1-4), 29-49 (1993).

9 LaTourrette, T., Hervig, R.L., & Holloway, J.R. Trace element partitioning between amphibole, phlogopite, and basanite melt. *Earth and Planetary Science Letters* **135**, 13-30 (1995).

10 Dalpe, C. & Baker, D.R. Experimental investigation of large-ion-lithophile-element-, high-field-strength-element- and rare-earth-element-partitioning between calcic amphibole and basaltic melt: the effects of pressure and oxygen fugacity. *Contributions to Mineralogy and Petrology* **140** (2), 233-250 (2000).

11 Wallace, M.E. & Green, D.H. The effect of bulk rock composition on the stability of amphibole in the upper mantle: Implications for solidus position and mantle metasomatism. *Mineralogy and Petrology* **44**, 1-19 (1991).

12 Class, C. & Goldstein, S.L. Plume-lithosphere interactions in the ccean basins: constraints from the source mineralogy. *Earth and Planetary Science Letters* **150**, 245-260 (1997).

13 Niida, K. & Green, D.H. Stability and chemical composition of pargasitic amphibole in MORB pyrolite under upper mantle conditions. *Contributions to Mineralogy and Petrology* **135** (1), 18-40 (1999).

14 Mertz, D. F., Devey, C. W., Todt, W., Stoffers, P., & Hofmann, A. W. Sr-Nd-Pb isotope evidece against plume asthenosphere mixing north of Icelan. *Earth and Planetary Science Letters* **107** (2), 243-255 (1991).

15 Mertz, D. F. & Haase, K. M. The radiogenic isotope composition of the high-latitude North Atlantic mantle. *Geology* **25** (5), 411-414 (1997).

16 Schilling, J.-G., Kingsley, R. H., Fontignie, D., Poreda, R., & Xue, S. Dispersion of the Jan Mayen and Iceland plumes in the Arctic: A He-Pb-Nd-Sr isotope tracer study of basalts from the Kolbeinsey, Mohns, and Knipovich Ridges. *Journal of Geophysical Research* **104** (B5), 10,543-510,569 (1999).

17 Blichert-Toft, J. *et al.* Geochemical segmentation of the Mid-Atlantic Ridge north of Iceland and ridge-hot spot interaction in the North Atlantic. *Geochemistry, Geophysics, Geosystems* **6** (Art. No. Q01E19) (2005).

18 Lehnert, K., Su, Y., Langmuir, C.H., Sarbas, B., & Nohl, U. A global geochemical database structure for rocks. *Geochemistry, Geophysics, Geosystems* **1**, doi:10.1029/1999GC000026 (2000).

19 Salters, V.J.M. & Stracke, A. Composition of the depleted mantle. *Geochemistry, Geophysics, Geosystems* **5**, #2003GC000597 (2004).

20 Workman, R.K. & Hart, S.R. Major and trace element composition of the depleted MORB mantle (DMM). *Earth and Planetary Science Letters* **231**, 53-72 (2005).